Available online at www.sciencedirect.com
SCIENCE DIRECT®
Journal of Computational Physics 199 (2004) 541–557
JOURNAL OF COMPUTATIONAL PHYSICS
www.elsevier.com/locate/jcp

A unified well-posed computational approach for the 2D Orr–Sommerfeld problem

Prashant G. Mehta *

Center for Applied Mathematics, Cornell University, Ithaca, NY 14850, USA

Received 3 September 2003; received in revised form 9 February 2004
Available online 24 March 2004

Abstract

In this paper, we present a unified well-posed implicit formulation for nonlinear 2D Orr–Sommerfeld equation (OSE) enabling straightforward, efficient computation of travelling wave and steady solutions. We illustrate the ease and utility of our approach by computing classical travelling wave results of planar Poiseuille flows and novel steady solutions of the perturbed planar Couette flow, employing the path-following software AUTO.

1. Introduction

In this paper, we consider the problem of computing travelling wave and steady solutions of the nonlinear Orr–Sommerfeld equation (OSE), cf. [1]. In particular, we present a formulation enabling straightforward, efficient computation of these solutions via standard path-following numerical techniques such as provided in AUTO [5]. At first glance the problem appears innocuous – continuation based travelling wave solutions of OSE can be found in papers as early as 1970s, see [22] for an early reference. However, the nonlinear (as well as the linear) problem of OSE, which we consider here, requires satisfaction of no-slip and impermeability boundary conditions on the channel walls. The no-slip boundary conditions occur as algebraic constraints to be satisfied for all values of the axial co-ordinate x on the channel walls. Here in lies the main difficulty – a travelling wave Hopf bifurcation problem after discretization becomes a differential algebraic equation (DAE) – not ideal for standard continuation softwares. A typical resolution to this is to discretize (in an a priori manner) the axial direction employing (usually) a Fourier basis and convert the problem in to a purely algebraic problem. This approach, however, yields an ill-posed system with more equations than unknowns and a standard resolution is to throw out certain high order algebraic equations so as to make the discrete system of algebraic equations square. We note that this difficulty is present even

* Present address: United Technologies Research Center, MS 15, UTRC, 411 Silver Lane, East Hartford, CT 06040, USA. Tel.: +1-860-610-7739.

E-mail address: mehtapg@utrc.utc.com (P.G. Mehta).

doi:10.1016/j.jcp.2004.02.018

in the linear problem (using collocation methods) and Chebyshev-tau method are used by introducing additional unknowns (τ) to make the discrete problem square, cf. [6]. The choice of Fourier bases also restricts the applicability of the method to periodic boundary conditions along the axial direction. We are not aware of any continuation studies that consider non-periodic boundary conditions for these problems.

Even though nonlinear solutions of OSE have been considered as early as Zahn et al. [22] and Herbert [10] in 1970s, the first uniform treatment for computing travelling wave solutions with OSE appears in the work of Milinazzo and Saffman [16]. The authors in this paper distinguish between the so-called uniform average flux and the uniform average pressure situations for computing nonlinear travelling wave solutions of parallel flows, and in particular of the planar Couette flow. With two Fourier modes, the authors were, however, unable to obtain these solutions for the planar Couette flow. The approach considered in [16] is further enunciated and used by Soibelman and Meiron [21], now with the purpose of computing travelling wave solutions for planar Poiseuille flow.

Cherhabili and Ehrenstein [3,4] – motivated by the work of Milinazzo and Saffman [16] – re-visit the problem of computing travelling wave solutions for planar Couette flow. The computational approach in [3] employs a Fourier basis to discretize the resulting 2D OSE along the axial direction with a view of obtaining an algebraic system of equations. In order to obtain a consistent set of equations, the authors use an average x-momentum equation when considering the zero-mode of the Fourier bases – see [3,7] for details on the discretization. The authors report that while they could not obtain solutions with two Fourier modes, they were successful in obtaining solutions for planar Couette flow with a larger set of Fourier modes. The authors also report appearance of localized structures and solutions that are nearly steady (wave speed of the travelling wave is small).

In addition to the above, there is vast body of literature on discretizing the linear OSE primarily with an objective of computing the spectrum, cf. [1] and the classical paper of Orszag [17] for an early reference. Most of the recent computational approaches are based either upon the Chebyshev collocation method [1,9,11] or the Chebyshev-tau method [1,6] and handle the boundary conditions explicitly. We note that the computations involving the nonlinear problem – as is the focus of this study – are more involved than the linear problem.

In this paper, we propose a Chebyshev collocation based approach for computing the continuation based nonlinear solution branches (and also the linear spectrum) of the 2D OSE. There are two principal ideas that make our approach novel. One, we use the formalism of Iooss et al. [13] and Iooss and Mielke [12] for *computing* the steady and travelling wave solutions, respectively, with OSE. As these papers do for the infinite-dimensional problem, we obtain a well-posed formulation for the discrete computational problem, while suitably satisfying the boundary conditions. In order to do so, however, we use an implicit scheme to appropriately fold the boundary conditions in – this constitutes the second novel idea of this paper. We show that after discretization, our approach results in a well-posed boundary value problem, whose solution may easily be obtained using standard path-following software such as AUTO. We note that our approach provides a well-posed formulation *independent* of the choice of discretization along the x-direction. Our approach also provides a unified framework for computing not only the travelling wave solutions – in both constant average flux and constant average pressure cases [16] – but also for computing certain steady wave solutions, where periodic boundary conditions may not necessarily apply.

The paper is organized as follows. In Section 2, we introduce the 2D OSE and contrast the objective of our computational formalism with more traditional approaches. In Section 3, we present the implicit approach for computing the travelling wave solutions, describing the discretized equations for both the constant average flux and the constant average pressure cases. In addition to the travelling wave solutions, we also motivate the problem of computing steady solutions of planar Couette flow. We show that on account of symmetry of the flow, computations must be carried out in a certain fixed-point-space. In this fixed-point-space, computations necessarily lead to non-periodic boundary conditions. For such a problem, we demonstrate the utility of our approach by obtaining a well-posed set of discretized equations quite simply. In Section 4, we validate the approach by replicating the standard linear spectrum, nonlinear local bifurcation results and continuation based travelling solutions for planar Poiseuille flow. We also use the framework outlined in Section 3 to compute certain steady solutions of the perturbed planar Couette flow. Finally in Section 5, we draw some conclusions.

2. Orr–Sommerfeld equation

The purpose of this section is to present the computational formalism of our approach. We begin by considering the two-dimensional (2D) incompressible Navier–Stokes Equation (NSE)

$$\frac{\partial \underline{u}}{\partial t} + (\underline{u}.\underline{\nabla})\underline{u} = -\underline{\nabla} p + \frac{1}{Re}\Delta \underline{u}, \tag{1}$$

$$\underline{\nabla}.\underline{u} = 0, \tag{2}$$

where $\underline{u} = (u, v)$ is the 2D velocity vector, $\underline{\nabla} = (\frac{\partial}{\partial x}, \frac{\partial}{\partial y})$ is the gradient vector, p is the scalar pressure field and Re is the Reynolds number. For bifurcation and continuation studies, it is useful to decompose the variables as

$$\underline{u} = \underline{U} + \underline{u}', \tag{3}$$

$$p = P + p', \tag{4}$$

where $(\underline{U}, P)$ is the basic solution and $(\underline{u}', p')$ is the perturbation. For parallel flows, $\underline{U} = (U(y), 0)$ and the NSE (1) and (2) is easily expressed in the perturbation co-ordinates (after dropping primes) as

$$\frac{\partial u}{\partial t} + U(y)\frac{\partial u}{\partial x} + U'(y)v + (\underline{u}.\underline{\nabla})u = -\frac{\partial p}{\partial x} + \frac{1}{Re}\Delta u, \tag{5}$$

$$\frac{\partial v}{\partial t} + U(y)\frac{\partial v}{\partial x} + (\underline{u}.\underline{\nabla})v = -\frac{\partial p}{\partial y} + \frac{1}{Re}\Delta v, \tag{6}$$

$$\underline{\nabla}.\underline{u} = 0. \tag{7}$$

For the 2D case, there exists a convenient co-ordinate change

$$u = \frac{\partial \Psi}{\partial y}, \quad v = -\frac{\partial \Psi}{\partial x} \tag{8}$$

which allows one to express the three Eqs. (5)–(7) in three variables (u, v, p) as a single equation in Ψ. Indeed the choice of the co-ordinate (8) automatically satisfies the divergence equation (7). Furthermore, on substituting the co-ordinate (8) in to the Eqs. (5) and (6) and taking the curl, one obtains the stream function formulation of NSE

$$\left(\frac{\partial}{\partial t} + U\frac{\partial}{\partial x}\right)\Delta\Psi - U''(y)\frac{\partial \Psi}{\partial x} - \frac{1}{Re}\Delta^2\Psi = -\left(\frac{\partial \Psi}{\partial y}\frac{\partial}{\partial x} - \frac{\partial \Psi}{\partial x}\frac{\partial}{\partial y}\right)\Delta\Psi. \tag{9}$$

The left-hand side of (9) is the linearization of the NSE (1) and (2) in Ψ co-ordinate and is referred to as the OSE. For our purpose, we shall refer to the complete equation (9) as the OSE simply using the prefix nonlinear in cases where confusion may likely arise as to which equation is meant. Needless to say, the linearization is used for computing the spectrum while the nonlinear OSE is used for continuation studies.

The OSE (9) is supplemented by boundary conditions which for channel (such as Poiseuille, Plane Couette) flows with boundaries at $y = \pm 1$ are

$$\text{No slip} \qquad u|_{y=\pm 1} = +\frac{\partial \Psi}{\partial y}\bigg|_{y=\pm 1} = 0 \quad \text{and} \quad \text{Impermeability} \qquad v|_{y=\pm 1} = -\frac{\partial \Psi}{\partial x}\bigg|_{y=\pm 1} = 0 \tag{10}$$

together with periodic boundary conditions in x-direction (for the case of bounded rectangular domain). A general solution of OSE (9) together with the boundary conditions (10) is $\Psi = \Psi(x, y, t)$. In this paper, we are most concerned with special solutions: (a) Steady where $\Psi = \Psi(x, y)$ and (b) Wave solutions where $\Psi = \Psi(x - ct, y)$ and c denotes the wave speed. Note that the steady solutions may be thought of as waves with speed $c = 0$. For these wave solutions expressed in the moving co-ordinate (x', y) with $x' = x - ct$, the OSE (9) becomes (after dropping primes)

$$\left(-c + U\frac{\partial}{\partial x}\right)\Delta\Psi - U''(y)\frac{\partial \Psi}{\partial x} - \frac{1}{Re}\Delta^2\Psi = -\left(\frac{\partial \Psi}{\partial y}\frac{\partial}{\partial x} - \frac{\partial \Psi}{\partial x}\frac{\partial}{\partial y}\right)\Delta\Psi. \tag{11}$$

In this paper, we formulate the computational problem for the wave OSE (11) together with its boundary conditions (10) as

$$\frac{\mathrm{d}\underline{a}}{\mathrm{d}x} = F(\underline{a}), \tag{12}$$

a 2-point boundary value problem in independent variable x. Here, the symbol $\underline{a}$ denotes a finite-dimensional representation of the streamfunction $\Psi[y](x)$ and its derivatives (along x). The bracket notation symbolizes the fact that Ψ is discretized along the y direction, but not along the axial direction. For instance, with the Chebyshev collocation method used in this paper, the discrete representation is merely the value of Ψ and of its axial derivatives at the collocation points. The symbol F denotes the finite-dimensional representation of the nonlinear OSE in the finite-dimensional co-ordinate $\underline{a}$. In the following sections, we provide details about this computational formalism.

Before doing so, however, we contrast the above formalism with the standard approach to discretizing the OSE. Typically, the OSE is converted in to a system of algebraic equations (see, for e.g. works of [3,21]) by choice of Fourier bases along the axial direction; periodic boundary conditions along the axial direction are assumed. Among the system of algebraic equations are the equations corresponding to the boundary conditions on the channel walls. In contrast, as described below, our boundary conditions are implicitly *folded* in to the right-hand side – nonlinear finite-dimensional operator F in Eq. (12). Our approach is quite independent of boundary conditions along the axial direction (and these need not be periodic). The non-periodic boundary conditions arise, for instance, in computations of steady solutions as described in Section 3.2. For the steady solutions, our computational approach in fact provides for a well-posed bifurcation and continuation scheme on an *unbounded* axial domain – *á la* theory of [13,14] – the steady solutions simply arise as a consequence of the Hopf bifurcation of (12) with unbounded co-ordinate x replacing the more standard time co-ordinate. As a result of these features, our approach provides for a unified 2-point boundary value framework for handling the computations of a class of OSE solutions.

3. Implicit discretization of the OSE

Computations with the linear and nonlinear problems associated with OSE (11) together with boundary condition (10) is the focus of the present section. After Iooss and Mielke [13], we express (11) as a differential equation in x-co-ordinate:

$$\frac{\partial \Psi}{\partial x} = \Psi_1, \tag{13}$$

$$\frac{\partial \Psi_1}{\partial x} = -\mathrm{D}^2\Psi + \Psi_2, \tag{14}$$

$$\frac{\partial \Psi_2}{\partial x} = \Psi_3, \tag{15}$$

$$\frac{1}{Re}\frac{\partial \Psi_3}{\partial x} = -\frac{1}{Re}\mathrm{D}^2\Psi_2 - (c-U)\Psi_3 - U''\Psi_1 + \{\mathrm{D}\Psi.\Psi_3 - \Psi_1.\mathrm{D}\Psi_2\}, \tag{16}$$

where the operator $\mathrm{D} \stackrel{\mathrm{def}}{=} \frac{\partial}{\partial y}$. The term in curly brackets is zero for the linear problem. Eqs. (13)–(16) together with the four boundary conditions:

$$\mathrm{D}\Psi(x, y = +1) = 0, \tag{17}$$

$$\mathrm{D}\Psi(x, y = -1) = 0, \tag{18}$$

$$\frac{\partial \Psi}{\partial x}(x, y = +1) = 0, \tag{19}$$

$$\frac{\partial \Psi}{\partial x}(x, y = -1) = 0 \tag{20}$$

constitute the system which needs to be discretized. For the steady problem, $c = 0$ and bifurcating steady nontrivial patterns arise when the linearization of (13)–(16) possesses eigenvalues that cross the imaginary axis. If the eigenvalue is real, the resulting steady pattern will be x-uniform and if the eigenvalues are imaginary then the pattern will show x-dependence related to the corresponding eigenfunction. For unsteady problem, c is a basic unknown and either domain length in x-direction needs to be fixed (and periodic boundary conditions imposed) or c may be a priori specified and wavelength of the solution allowed to vary.

A popular strategy to discretize the differential equations (13)–(16) together with boundary conditions (17)–(20) is the so-called Chebyshev collocation method [1], where each of the continuous functions $(\Psi(y), \Psi_1(y), \Psi_2(y), \Psi_3(y))$ are represented by their discrete values $(\Psi[j], \Psi_1[j], \Psi_2[j], \Psi_3[j])$ at the collocation grid points

$$y_j = \cos\left(\frac{\pi j}{N}\right), \quad j = 0, 1, \ldots, N \tag{21}$$

and the derivative D of variables in the right-hand side of Eqs. (13)–(16) and in boundary equations (17)–(20) is evaluated at these grid points as (or in a manner analogous to)

$$\mathrm{D}\Psi(y_i) = \sum_{j=0}^{N} (\mathbb{D}_N)_{lj} \Psi(y_j), \tag{22}$$

where $\mathbb{D}$ is the Chebyshev collocation differentiation matrix [1]. The computational problem is to obtain the values of Ψ at the $N+1$ discrete grid points in (21) – a total of $N+1$ unknowns $\Psi[j],\ j = 0, \ldots, N$ whose differential equation (using (13)) is

$$\frac{\partial \Psi[j]}{\partial x} = \Psi_1[j], \quad 0 \leqslant j \leqslant N \tag{23}$$

and whose solution requires knowledge of Ψ_1 and hence the solution of the corresponding differential equation (using (14))

$$\frac{\partial \Psi_1[j]}{\partial x} = -\mathrm{D}^2\Psi[j] + \Psi_2[j], \quad 0 \leqslant j \leqslant N \tag{24}$$

where $\mathrm{D}^2\Psi[j]$ denotes the values of $\mathrm{D}^2\Psi$ evaluated at the jth collocation grid point and the differential equation for Ψ_2 (using (15)) is given by

$$\frac{\partial \Psi_2[j]}{\partial x} = \Psi_3[j], \quad 0 \leqslant j \leqslant N \tag{25}$$

for a total of $3(N+1)$ equations in $4(N+1)$ unknowns (values of $(\Psi[j], \Psi_1[j], \Psi_2[j], \Psi_3[j])$ for $0 \leqslant j \leqslant N$). The OSE (16) solved at N interior collocation points

$$\begin{aligned} \frac{1}{Re}\frac{\partial \Psi_3[j]}{\partial x} = & -\frac{1}{Re}\mathrm{D}^2\Psi_2[j] - (c-U)\Psi_3[j] - U''[j]\Psi_1[j] \\ & + \{\mathrm{D}\Psi[j]\ \Psi_3[j] - \Psi_1[j]\ D\Psi_2[j]\}, \quad 1 \leqslant j \leqslant N-1 \end{aligned} \tag{26}$$

together with the boundary conditions (17) and (18)

$$\frac{\partial \Psi[0]}{\partial x} = 0, \tag{27}$$

$$\frac{\partial \Psi[N]}{\partial x} = 0 \tag{28}$$

provide the extra $(N+1)$ differential equations thereby yielding $4(N+1)$ equations in as many unknowns. The problem with this approach is the solution thus found need not satisfy the algebraic boundary conditions arising from (19) to (20)

$$\mathrm{D}\Psi[0](x) = 0, \tag{29}$$

$$\mathrm{D}\Psi[N](x) = 0. \tag{30}$$

So, the complete system whose solution we would like to determine is the DAE (Eqs. (23)–(30)). We note that the algebraic equations (29) and (30) must be satisfied for all x in the domain.

One possible resolution to to the above problem is to express the $\Psi[j](x)$ in Fourier bases thereby converting the entire system in to an algebraic problem. This is the spirit of analysis done by several authors including [3,21]. However, we are interested in obtaining a formulation consisting of differential equations only with the purpose of using AUTO for continuation of nonlinear solutions. For this purpose, we propose an implicit formulation of the problem where the Neumann boundary conditions (29) and (30) are folded into the differential equation.

The implicit formulation works by replacing the $\mathrm{D}\Psi$ terms on the right-hand side of differential equations (23)–(26) by $\hat{\mathrm{D}}\Psi$ where

$$\hat{\mathrm{D}} = \begin{bmatrix} 0\cdots 0 \\ \mathrm{D}(2:N,:) \\ 0\cdots 0 \end{bmatrix}. \tag{31}$$

The implicit approach has been suggested by [1] for the linear problem (where nonlinear terms on right-hand side of Eq. (11) are absent). We note, however, that the implicit approach does not buy a whole lot for the linear problem because of the relative ease of handling the linear problem using Fourier bases (where the individual modal components decouple). However, for the nonlinear problem, all of the different Fourier modal components are coupled (in a convolution manner) due to the nonlinear product term on the right-hand side of (11). This makes the approach presented below ideal for the nonlinear continuation problems.

The boundary conditions (27) and (28) set the values of

$$\Psi_1[j] = 0, \quad j = 0, N, \tag{32}$$

We thus have $N-1$ differential equations defining $\Psi_1[j]$ at interior collocation points (using (23))

$$\frac{\partial \Psi[j]}{\partial x} = \Psi_1[j], \quad 1 \leqslant j \leqslant N-1. \tag{33}$$

Eq. (24) now defines Ψ_2 as $N-1$ interior collocation points with the implicit modification given as

$$\frac{\partial \Psi_1[j]}{\partial x} = -\mathrm{D}\hat{\mathrm{D}}\Psi[j] + \Psi_2[j], \quad 1 \leqslant j \leqslant N-1 \tag{34}$$

and due to (32), we have

$$\Psi_2[j](x) = \mathrm{D}\hat{\mathrm{D}}\Psi[j](x), \quad j = 0, N. \tag{35}$$

As before in (25), we have (now only at interior collocation points)

$$\frac{\partial \Psi_2[j]}{\partial x} = \Psi_3[j], \quad 1 \leqslant j \leqslant N-1. \tag{36}$$

and the OSE (26) becomes

$$\begin{aligned} \frac{1}{Re}\frac{\partial \Psi_3[j]}{\partial x} = {} & -\frac{1}{Re}\mathrm{D}^2\Psi_2[j] - \left[\frac{1}{Re}\mathrm{D}^2(j,[0,N])\Psi_2([0,N])\right] - (c-U)\Psi_3[j] - U''[j]\Psi_1[j] \\ & + \{\mathrm{D}\Psi[j]\Psi_3[j] - \Psi_1[j]D\Psi_2[j] - [\Psi_1[j]\mathrm{D}(j,[0,N])\Psi_2([0,N])]\}, \quad 1 \leqslant j \leqslant N-1 \end{aligned} \tag{37}$$

where the terms in square brackets are the corrector terms that arise due to (35) and capture the contribution of $\Psi_2[0]$ and $\Psi_2[N]$ on the OSE. Finally, we note that the two boundary conditions (27) and (28) yield $\Psi[j](x)$ for $j = 0, N$ to be constants

$$\Psi[j](x) = C_j, \quad j = 0, N \tag{38}$$

to be shortly set. Since, Ψ is uniquely defined only up to a constant, we arbitrarily set $C_0 = 0$, i.e.,

$$\Psi[0] = 0. \tag{39}$$

To define C_N uniquely, we require an extra condition. The indeterminacy arises due to the arbitrariness in the choice of the basic flow velocity [21]. There are two ways discussed in literature to impose this extra condition [16]. Below, we discuss the implicit formulation in either cases, showing each case to yield a well-posed boundary value problem.

3.1. Travelling wave solutions

One way to impose the extra condition is to require no perturbation to the average flux [21], i.e.,

$$\int_0^L \int_{-1}^1 u \,\mathrm{d}y \,\mathrm{d}x, \tag{40}$$

which after substituting the definition for streamfunction yields

$$C_N = C_0, \tag{41}$$

i.e.,

$$\Psi[N] = 0. \tag{42}$$

This gives rise to the following $4(N-1)$ differential equations:

$$\frac{\partial \Psi[j]}{\partial x} = \Psi_1[j], \quad 1 \leqslant j \leqslant N-1, \tag{43}$$

$$\frac{\partial \Psi_1[j]}{\partial x} = -\mathrm{D}\hat{\mathrm{D}}(j, 1:N-1)\Psi + \Psi_2[j], \quad 1 \leqslant j \leqslant N-1, \tag{44}$$

$$\frac{\partial \Psi_2[j]}{\partial x} = \Psi_3[j], \quad 1 \leqslant j \leqslant N-1, \tag{45}$$

$$\begin{aligned}\frac{1}{Re}\frac{\partial \Psi_3[j]}{\partial x} = & -\frac{1}{Re}\mathrm{D}^2(j, 1:N-1)\Psi_2 - \left[\frac{1}{Re}\mathrm{D}^2(j,[0,N])\mathrm{D}\hat{\mathrm{D}}([0,N], 1:N-1)\Psi\right] \\ & - (c-U)\Psi_3[j] - U''[j]\Psi_1[j] + \Big\{\mathrm{D}(j, 1:N-1)\Psi\Psi_3[j] - \Psi_1[j]\mathrm{D}(j, 1:N-1)\Psi_2 \\ & - \Big[\Psi_1[j]\mathrm{D}(j,[0,N])\mathrm{D}\hat{\mathrm{D}}([0,N], 1:N-1)\Psi\Big]\Big\}, \quad 1 \leqslant j \leqslant N-1\end{aligned} \tag{46}$$

in $4(N-1)$ unknowns – values of $(\Psi[j], \Psi_1[j], \Psi_2[j], \Psi_3[j])$ at the $N-1$ interior collocation grid points given by (21). The boundary conditions have been incorporated implicitly in to the formulation. The term in the curly brackets is zero for the linear problem and the terms in square brackets are the corrector terms.

The second way to impose the extra condition is to require no perturbation to the average pressure which leads to (see [21])

$$\int_0^L \frac{\partial^2 \Psi}{\partial y^2}(y=+1, x) - \frac{\partial^2 \Psi}{\partial y^2}(y=-1, x)\,\mathrm{d}x = 0. \tag{47}$$

Using the implicit notation, this implies

$$\int_0^L \mathrm{D}\hat{\mathrm{D}}\Psi[0](x) - \mathrm{D}\hat{\mathrm{D}}\Psi[N](x) = 0. \tag{48}$$

Therefore,

$$\int_0^L \Psi_2[0](x) - \Psi_2[N](x)\,\mathrm{d}x = 0. \tag{49}$$

Since C_N is a non-zero unknown in the zero average pressure condition above, we are led to the following $4(N-1)$ differential equations:

$$\frac{\partial \Psi[j]}{\partial x} = \Psi_1[j], \quad 1 \leqslant j \leqslant N-1, \tag{50}$$

$$\frac{\partial \Psi_1[j]}{\partial x} = -\mathrm{D}\hat{\mathrm{D}}(j, 1:N-1)\Psi - \mathrm{D}\hat{\mathrm{D}}(j, N)C_N + \Psi_2[j], \quad 1 \leqslant j \leqslant N-1, \tag{51}$$

$$\frac{\partial \Psi_2[j]}{\partial x} = \Psi_3[j], \quad 1 \leqslant j \leqslant N-1, \tag{52}$$

$$\begin{aligned}\frac{1}{Re}\frac{\partial \Psi_3[j]}{\partial x} = &-\frac{1}{Re}\mathrm{D}^2(j, 1:N-1)\Psi_2 - \Big[\frac{1}{Re}\mathrm{D}^2(j, [0,N])\mathrm{D}\hat{\mathrm{D}}([0,N], 1:N-1)\Psi \\ &-\frac{1}{Re}\mathrm{D}^2(j, [0,N])\mathrm{D}\hat{\mathrm{D}}([0,N], N)C_N\Big] - (c-U)\Psi_3[j] \\ &- U''[j]\Psi_1[j] + \Big\{\mathrm{D}(j, 1:N-1)\Psi\Psi_3[j] \\ &- \Psi_1[j]\mathrm{D}(j, 1:N-1)\Psi_2 - \Big[\Psi_1[j]\mathrm{D}(j,[0,N])\mathrm{D}\hat{\mathrm{D}}([0,N], 1:N-1)\Psi \\ &+ \Psi_1[j]\mathrm{D}(j,[0,N])\mathrm{D}\hat{\mathrm{D}}([0,N],N)C_N\Big]\Big\}, \quad 1 \leqslant j \leqslant N-1\end{aligned} \tag{53}$$

in $4(N-1)+1$ unknowns – values of $(\Psi[j], \Psi_1[j], \Psi_2[j], \Psi_3[j])$ at the $N-1$ interior collocation grid points given by (21) and the unknown constant C_N. The integral zero average pressure condition

$$\int_0^L \Psi_2[0](x) - \Psi_2[N](x)\,\mathrm{d}x = 0 \tag{54}$$

is the extra equation for the resulting constrained system of equations to be well-posed.

Both the zero average flux case (Eqs. (43)–(46)) as well as the zero average pressure case (Eqs. (50)–(53)) together with the integral constraint (54)) yield a well-posed formulation for carrying out computations of the travelling wave solutions. Moreover, the 2-point BVP framework allows standard continuation codes such as AUTO [5] to be easily used for computing these solutions.

3.2. Steady solutions

In addition to the travelling wave solutions, we also use the above formulation to compute steady solutions. For problems with SO(2) spatial symmetry along the axial direction (e.g. planar Poiseuille flow), the computations of steady solutions are straightforward. One merely chooses $c = 0$ and the steady solutions arise simply as the spatial Hopf bifurcation – with the co-ordinate x substituting for the more familiar time t. In this context, the framework outlined for the travelling wave solutions above applies – for both constant average flux and average pressure cases. However, for many problems in fluid dynamics (for e.g. planar Couette flow), the presence of large (O(2) in the case of planar Couette flow) symmetry group leads to the presence of multi-dimensional eigenspace [20] at the bifurcation point. For such problems, fixed-point-space computations are necessary for obtaining isolated solution branches using standard continuation schemes such as AUTO. In a fixed-point-space, however, the periodic boundary conditions need not apply and it is here, the unified boundary value problem framework developed in this paper becomes useful. Below, we present these ideas for the special case of planar Couette flow.

The equations of motion for the planar Couette flow are O(2) (spatial symmetry group) equivariant [15]. In the streamfunction co-ordinate, the symmetry group induces an action

$$SO(2) : \tau_a[\Psi(x,y)] = \Psi(x+a,y) \quad \forall a \in \mathbb{R} (\text{mod } 2\pi) \tag{55}$$

$$Z^2 : \sigma[\Psi(x,y)] = \Psi(-x,-y). \tag{56}$$

The presence of O(2) symmetry group leads to the occurrence of a multi-dimensional eigenspace at the bifurcation point, if indeed such a point exists. For the unsteady O(2) Hopf situation, the symmetry leads to two pairs of imaginary eigenvalues – corresponding to forward and backward travelling waves. For the steady O(2) bifurcation problem, the symmetry leads to double real eigenvalues. The occurrence of multiple eigenvalues requires fixed-point-space computations in order to compute an isolated branch of solutions. Below, we describe such a framework for computing steady solutions, i.e., solutions such that

$$\frac{\partial}{\partial t} = 0, \tag{57}$$

and the streamfunction

$$\Psi = \Psi(x,y). \tag{58}$$

For the O(2) equivariant group, the fixed-point-space corresponding to the isotropy subgroup Z^2 yields an isolated branch of solution [8]. Using Eq. (56), the Z^2 fixed-point-space may be defined as the space of functions satisfying

$$\Psi(x,y) = \Psi(-x,-y), \tag{59}$$

on the rectangular domain $[-\frac{L}{2},\frac{L}{2}] \times [-1,1]$. The pattern resulting from (59) is schematically drawn in Fig. 1. We may carry out the fixed-point-space computations on the half-domain $[0,\frac{L}{2}] \times [-1,1]$ either using zero average flux equations (43)–(46) or the zero average pressure equations (50)–(53). In either case, the periodic boundary conditions along the x-direction are replaced by the boundary conditions consistent with the pattern (59). These boundary conditions for the continuous problem are given by

$$\Psi(x=0,y) = \Psi(x=0,-y) \quad \forall y \in (0,1), \tag{60}$$

$$\Psi\left(x=\frac{L}{2},y\right) = \Psi\left(x=\frac{L}{2},-y\right) \quad \forall y \in (0,1), \tag{61}$$

$$\Psi_x(x=0,y) = -\Psi_x(x=0,-y) \quad \forall y \in (0,1), \tag{62}$$

$$\Psi_x\left(x=\frac{L}{2},y\right) = -\Psi_x\left(x=\frac{L}{2},-y\right) \quad \forall y \in (0,1), \tag{63}$$

$$\Psi_x(x=0,y=0) = 0, \tag{64}$$

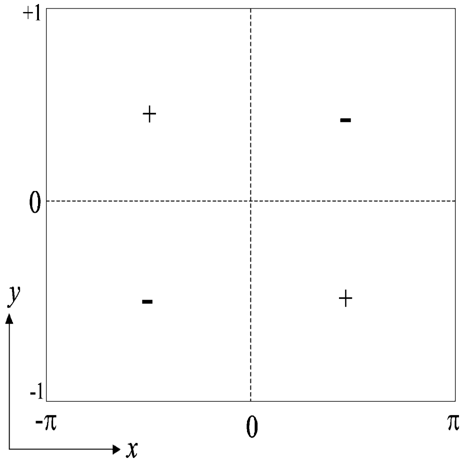

Fig. 1. Z^2 symmetric pattern satisfying Eq. (59).

$$\Psi_x\left(x=\frac{L}{2},y=0\right)=0, \tag{65}$$

$$\Delta\Psi(x=0,y)=\Delta\Psi(x=0,-y)\quad\forall y\in(0,1), \tag{66}$$

$$\Delta\Psi\left(x=\frac{L}{2},y\right)=\Delta\Psi\left(x=\frac{L}{2},-y\right)\quad\forall y\in(0,1), \tag{67}$$

$$\Delta\Psi_x(x=0,y)=-\Delta\Psi_x(x=0,-y)\quad\forall y\in(0,1), \tag{68}$$

$$\Delta\Psi_x\left(x=\frac{L}{2},y\right)=-\Delta\Psi_x\left(x=\frac{L}{2},-y\right)\quad\forall y\in(0,1), \tag{69}$$

$$\Delta\Psi_x(x=0,y=0)=0, \tag{70}$$

$$\Delta\Psi_x(x=\frac{L}{2},y=0)=0. \tag{71}$$

The boundary conditions for the discrete problem with N collocation points are:

$$\Psi[j](x=0)=\Psi[N-j](x=0), \tag{72}$$

$$\Psi[j]\left(x=\frac{L}{2}\right)=\Psi[N-j]\left(x=\frac{L}{2}\right), \tag{73}$$

$$\Psi_1[j](x=0)=-\Psi_1[N-j](x=0), \tag{74}$$

$$\Psi_1[j]\left(x=\frac{L}{2}\right)=-\Psi_1[N-j]\left(x=\frac{L}{2}\right), \tag{75}$$

$$\Psi_2[j](x=0) = \Psi_2[N-j](x=0), \tag{76}$$

$$\Psi_2[j]\left(x=\frac{L}{2}\right) = \Psi_2[N-j]\left(x=\frac{L}{2}\right), \tag{77}$$

$$\Psi_3[j](x=0) = -\Psi_3[N-j](x=0), \tag{78}$$

$$\Psi_3[j]\left(x=\frac{L}{2}\right) = -\Psi_3[N-j]\left(x=\frac{L}{2}\right). \tag{79}$$

For an odd value of N, $j = 1, \ldots, \frac{N-1}{2}$ and the above boundary conditions suffice. However, for an even value of N, $j = 1, \ldots, \frac{N}{2} - 1$ and we have the following extra boundary conditions:

$$\Psi_1\left[\frac{N}{2}\right](x=0) = 0, \tag{80}$$

$$\Psi_1\left[\frac{N}{2}\right]\left(x=\frac{L}{2}\right) = 0, \tag{81}$$

$$\Psi_3\left[\frac{N}{2}\right](x=0) = 0, \tag{82}$$

$$\Psi_3\left[\frac{N}{2}\right]\left(x=\frac{L}{2}\right) = 0. \tag{83}$$

In either case, a well-posed boundary value problem results with as many boundary conditions as the $4 \times N - 4$ ODE (43)–(46).

In the following section, we present some examples meant to validate the formulation (43)–(46) presented above with some published results. For the nonlinear bifurcation and continuation studies, the program AUTO [5] was used. A detailed code listing for this together with a computational guide including discussion on computational issues appears in [15].

4. Examples

We present results computed using Eqs. (43)–(46) for the following three examples:

4.1. Linear spectrum example

In this example, we compute the linear spectrum of Plane Couette flow and compare it against the results of [6]. Fig. 2 plots the numerically computed spectrum at $Re = 3500$, $\alpha = 1$ using $K = 200$ Chebyshev modes. These computations are carried out in MATLAB using 64 bit arithmetic. The choice of the Reynolds number is due to the fact that above $Re = 3500$, the computation of eigenvalues breaks down. Even at the Reynolds number of 3500, as seen in the figure, the so-called tail of the spectrum (where the eigenvalues are expected to have zero imaginary part) shows discrepancies from the expected solution. This observations are consistent with [6] who reported similar behavior with 64 bit arithmetic. In Table 1, we compare the eigenvalues obtained with the implicit method, now for $Re = 13{,}000$, to those reported in [6] for the first

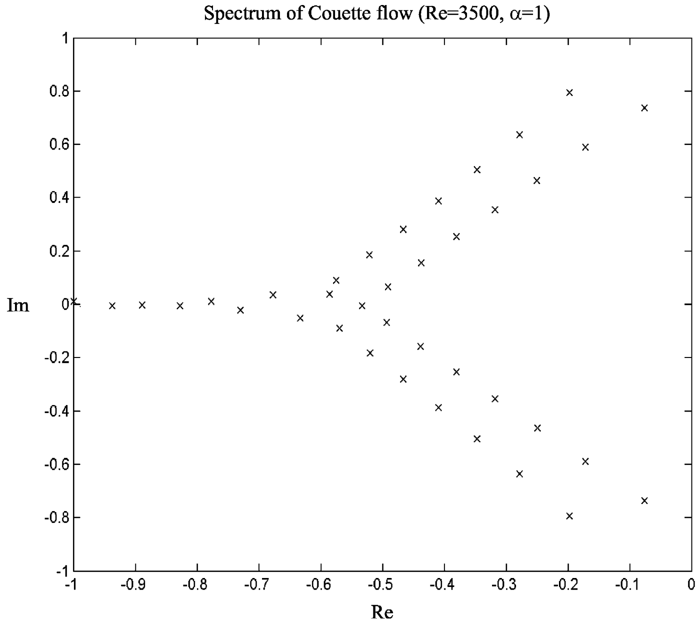

Fig. 2. Numerically computed spectrum of planar Couette flow at $Re = 3500$, $\alpha = 1$ using $K = 200$ Chebyshev modes.

Table 1
The first 15 eigenvalues compared with Dongarra's results [6] ($K = 200$, $Re = 13{,}000$, $\alpha = 1$)

#	Eigenvalue (64 bit computations)	Dongarra's eigenvalue [6] (128 bit)
1	−0.04751565735 ± 0.82761545888i	−0.04751548439 ± 0.8276152337i
2	0.10916233090 ± 0.73179748710i	−0.1091860424 ± 0.7318167785i
3	0.12788692688 ± 0.86944989709i	−0.1279149536 ± 0.8694486153i
4	0.15940221500 ± 0.65168384313i	−0.1594003003 ± 0.6516804277i
5	0.18053506749 ± 0.76712088000i	−0.1805164930 ± 0.7671186628i
6	0.20355912367 ± 0.58016155986i	−0.2035572830 ± 0.5801567166i
7	0.22517251154 ± 0.68283374656i	−0.2251746419 ± 0.6828371673i
8	0.24374083416 ± 0.51444025167i	−0.2437675825 ± 0.5143995235i
9	0.26531490806 ± 0.60811869339i	−0.2653481107 ± 0.6082408213i
10	0.28115172316 ± 0.45299528229i	−0.2811241939 ± 0.4528935800i
11	0.30216857441 ± 0.54001675911i	−0.3024678732 ± 0.5400219613i
12	0.31629839110 ± 0.39473406600i	−0.3162828159 ± 0.3947096982i
13	0.33723447385 ± 0.47637056686i	−0.3373108149 ± 0.4764491821i
14	0.34646662472 ± 0.31977167963i	−0.3496747907 ± 0.3392256967i
15	0.34744532686 ± 0.27061969756i	−0.3703603829 ± 0.4164746866i

14 modes which we are able to compute satisfactorily. For the purposes of comparison, we adapted the method described above to be consistent with the so-called D^2 method used in [6].

4.2. Weak nonlinear analysis example

In this example, we present the computational results determining the so-called Landau constant using the Joseph–Sattinger perturbation series method [19] for the local analysis of the first bifurcation point of planar Poiseuille flow. We compare these results with the results of [2]. Fig. 3 plots the spectrum of the

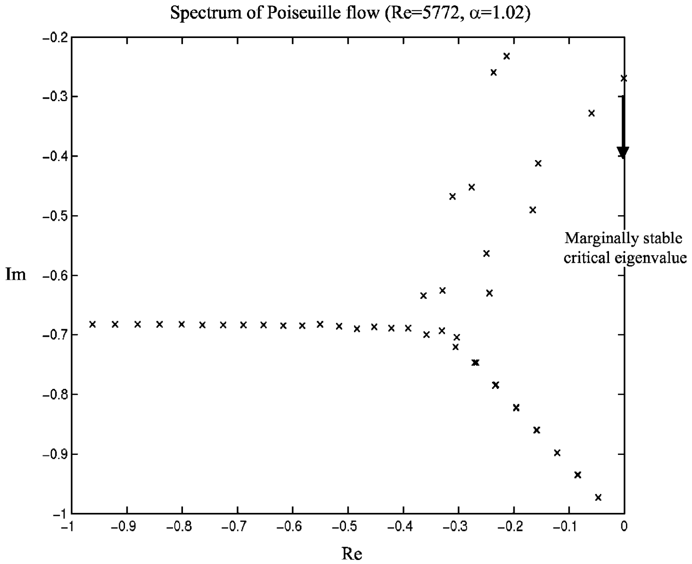

Fig. 3. Numerically computed spectrum of planar Poiseuille flow at the critical Reynolds number $Re = 5772$, $\alpha = 1.02$ using $K = 200$ Chebyshev modes.

Planar Poiseuille flow for the critical Reynolds number $Re = 5772$, where the basic parallel flow solution loses stability and undergoes a Hopf bifurcation thereby yielding a subcritical travelling wave solution. For this travelling wave solution, a perturbation series is constructed using the Joseph–Sattinger method and the computations are carried out using the computational formulation described in Section 3.1. Table 2 compares the numerical results with the results of [2]: c is the wave speed, ζ' is the speed at which the real part of the eigenvalue crosses the imaginary axis, λ_2 is the Landau constant and ω_2 is the value for the nonlinear perturbation of frequency along the bifurcating branch.

4.3. Continuation for travelling wave solution

In this example, we use AUTO to continue globally the primary bifurcating branch of the Planar Poiseuille flow. Fig. 4 plots the wave speed c of the bifurcating solution against the Reynolds number. The bifurcating solution is subcritical, consistent with the analysis above. The bifurcating branch shows a limit point at Reynolds number of about 4400, consistent with the computations of [22].

4.4. Continuation for steady solution

The purpose of this section is to present results utilizing the fixed-point-space computational framework discussed in Section 3.2. The framework presented therein was primarily motivated for continuing steady solutions of planar Couette flow, which has an O(2) symmetry group. However, though the planar Couette

Table 2
Summary of the weak nonlinear analysis computations for the planar Poiseuille flow's primary bifurcating branch

Implicit computations				Chen and Joseph [2]			
c	ζ'	λ_2	ω_2	c	ζ'	λ_2	ω_2
0.2692	56.18	0.499	304.54	0.2640	56.10	0.556	323.42

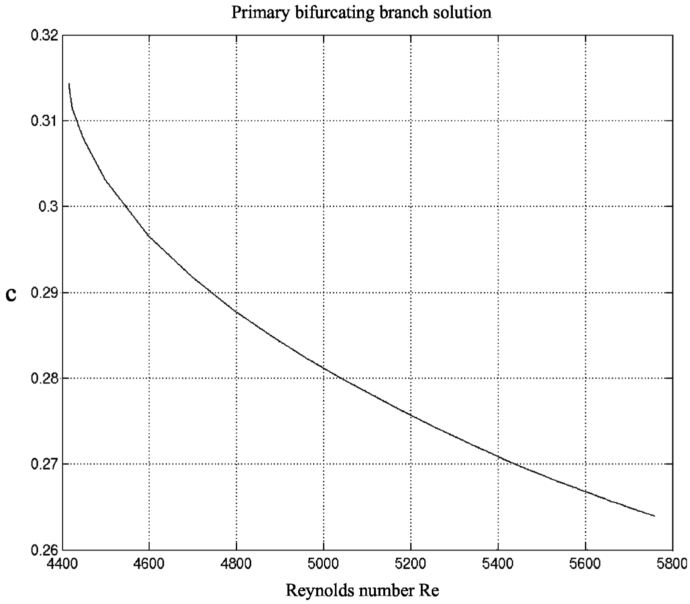

Fig. 4. Wave speed $c(Re)$ of the primary bifurcating travelling wave branch for planar Poiseuille flow.

flow has real eigenvalues, they remain in the left half plane for all finite values of Reynolds number [18], and as a result the basic laminar solution does not bifurcate.

In order to cause the planar Couette flow to bifurcate, we perturb it with the objective of causing one of the real eigenvalues to cross the imaginary axis. Perturbations that cause the planar Couette flow to bifurcate

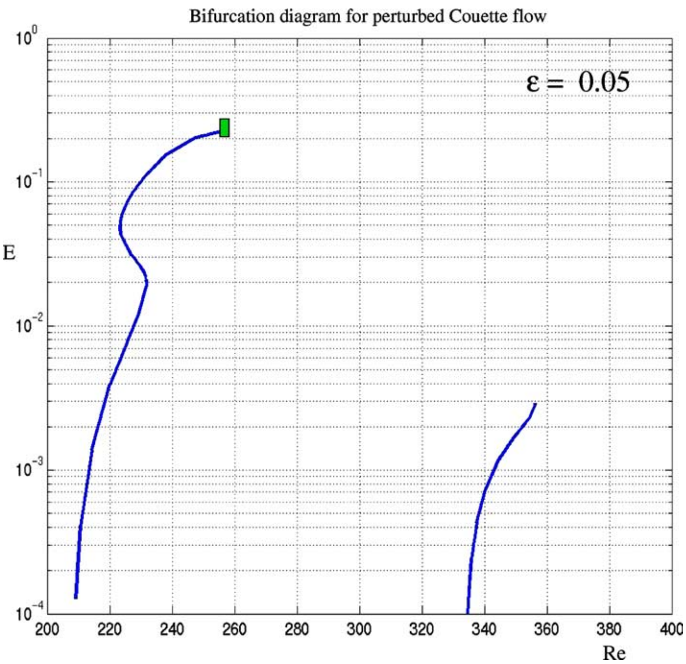

Fig. 5. Bifurcation diagram for perturbed planar Couette flow.

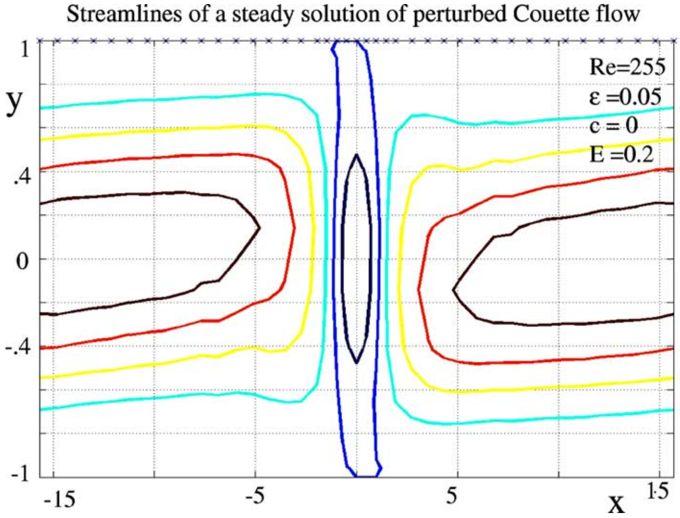

Fig. 6. Streamlines for perturbed planar Couette flow for $\epsilon = 0.05$, $Re = 255$: 'x' denote the collocation points along the axial direction. Note the cluster around the localized structure which is resolved by the computational method.

have been considered before in [3,16], who used a Poiseuille–Couette homotopy to perturb the planar Couette flow. However, this homotopy destroys the O(2) equivariance of the planar Couette flow. In order to preserve the O(2) equivariance and still cause the flow to bifurcate, we use an identity homotopy that perturbs the Navier–Stokes equations by simply adding ϵI. The homotopy parameter ϵ is chosen to be suitably large so as to cause a real eigenvalue to cross the imaginary axis for a finite value of Reynolds number [15].

Fig. 5 depicts the bifurcation diagram for a choice of identity perturbation with $\epsilon = 0.05$ and $\alpha = 0.2$. The steady solutions were obtained by detecting bifurcation (for the perturbed planar Couette flow) and continuing along the fixed-point-space using the framework described in Section 3.2. Fig. 6 presents the streamlines for a solution along the bifurcating branch. It shows the presence of localized structures of the kind described in the work of [3] and the computational technique used adaptive meshing along the axial direction (available in AUTO) to resolve these structures accurately. Additional details on the structure of steady solutions of perturbed Couette flow and their relation to the planar Couette flow appear in [15] and will be presented separately.

5. Conclusion

In this paper, we have presented a unified approach for computing travelling wave and steady solutions of parallel flow problems using continuation methods. The computational framework developed in this paper yields a well-posed two point boundary value problem suitable for detecting bifurcations and carrying out continuation with AUTO.

Compared to standard approaches which employ Fourier bases to discretize the equation along the axial direction, the method is more general and offers several advantages. Apart from its ability to handle non-periodic boundary conditions, its greatest advantage is the ease with which the equations of motion may be used in AUTO. Once the Chebyshev collocation differentiation matrix is computed, specifying the right-hand side of the boundary value problem for either the constant flux case equations (43)–(46) or the zero average pressure case equations (50)–(53) can be implemented using four *straightforward* loops. Continuation schemes such as AUTO also allow for symbolic representation of Jacobian and derivatives with respect to parameters, which too are straightforward (about an arbitrary nonlinear solution) to obtain –

simply take the Jacobian of the right-hand side. In contrast, representation and coding the nonlinear terms (which arise as a consequence of convolution) after using Fourier bases is much more cumbersome. Our approach is easier because the product nature of the nonlinearity present in the original equations is preserved in the discretized equations.

Finally, the localized structures such as shown in Fig. 6 have been seen in computations of [3] and difficult to resolve using Fourier bases; see also [16] and discussion in [3] on the sensitivity of solutions to the number of Fourier bases. For this purpose, if not other, continuation approaches such as AUTO which employ (user transparent) collocation methods for discretization and adaptive griding are useful to continue solutions with localized structures: our approach is tailor-made to harness this power.

Acknowledgements

I acknowledge Prof. Timothy J. Healey for many useful discussions and for his guidance during the course of this work.

References

[1] C. Canuto, M.Y. Hussaini, A. Quarteroni, T.A. Zang, Spectral Methods in Fluid Dynamics, Springer Series in Computational Physics, Springer, New York, 1983.
[2] T.S. Chen, D.D. Joseph, Subcritical bifurcation in planar Poiseuille flow, Journal of Fluid Mechanics 58 (1973) 337–351.
[3] A. Cherhabili, U. Ehrenstein, Spatially localized two-dimensional finite-amplitude states in plane Couette flow, European Journal of Mechanics B/Fluids 14 (1995) 677–696.
[4] A. Cherhabili, U. Ehrenstein, Finite-amplitude equilibrium states in plane Couette flow, Journal of Fluid Mechanics 342 (1997) 159–177.
[5] E.J. Doedel, Auto2000: continuation and bifurcation software for ordinary differential equations, 2000.
[6] J.J. Dongarra, B. Straughan, D.W. Walker, Chebyshev tau-qz algorithm methods for calculating spectra of hydrodynamic stability problems, Applied Numerical Mathematics 22 (1996) 399–434.
[7] U. Ehrenstein, The spectrum of Chebyshev Fourier approximation for the Stokes equation, Journal of Scientific Computing (1990) 55–84.
[8] M. Golubitsky, I. Stewart, D.G. Schaeffer, in: Singularities and Groups in Bifurcation Theory, vol. II, Springer, New York, 1988.
[9] T. Herbert, Die neutrale flache der ebenen Poiseuille–Stromung. Habilitation, University of Stuttgart, 1977.
[10] T. Herbert, Stability of plane Poiseuille flow – theory and experiments, Fluid Dynamics and Transactions 11 (1981) 77–126.
[11] W. Huang, D.M. Sloan, The pseudospectral method for solving differential eigenvalue problems, Journal of Computational Physics 111 (1994) 399–409.
[12] G. Iooss, A. Mielke, Bifurcating time-periodic solutions of Navier–Stokes equations in infinite cylinders, Journal of Nonlinear Science 1 (1991) 107–146.
[13] G. Iooss, A. Mielke, Y. Demay, Theory of steady Ginzburg–Landau equation in hydrodynamics stability problems, Journal of Nonlinear Science 1 (1989) 106–146.
[14] K. Kirchgässner, Wave-solutions of reversible systems and applications, Journal of Differential Equations 45 (1982) 113–127.
[15] P.G. Mehta, Nonbifurcating solutions for parallel flows, Ph.D. Thesis, Cornell University, 2004.
[16] F.A. Milinazzo, P.G. Saffman, Finite-amplitude steady waves in plane viscous shear flows, Journal of Fluid Mechanics 160 (1985) 280–295.
[17] S.A. Orszag, Accurate solution of the Orr–Sommerfeld stability equation, Journal of Fluid Mechanics 50 (4) (1971) 689–703.
[18] V.A. Romanov, Stability of plane-parallel Couette flow, Functional Analysis and its Applications 7 (1973) 137–146.
[19] D.H. Sattinger, Topics in Stability and Bifurcation Theory, Lecture notes in Mathematics, Springer, Berlin, 1983, 1973.
[20] D.H. Sattinger, Group representation theory, bifurcation theory and pattern formation, Journal of Functional Analysis 28 (1978) 58–101.
[21] I. Soibelman, D.I. Meiron, Finite-amplitude bifurcations in plane Poiseuille flow: two-dimensional bifurcation, Journal of Fluid Mechanics 229 (1991) 389–416.
[22] J.P. Zahn, J. Toomre, E.A. Speigel, D.O. Gough, Nonlinear cellular motion in Poiseuille channel flow, Journal of Fluid Mechanics 64 (1974) 319–345.